Eur. Phys. J. C (2025) 85:1149
https://doi.org/10.1140/epjc/s10052-025-14909-0

THE EUROPEAN PHYSICAL JOURNAL C

Regular Article - Theoretical Physics

Thermodynamics and Joule–Thomson expansion of Schwarzschild-AdS black holes with a cloud of strings and quintessential-like fluid

Faizuddin Ahmed[1,a], **Saeed Noori Gashti**[2,b], **Behnam Pourhassan**[2,3,c], **Abdelmalek Bouzenada**[4,d]

[1] Department of Physics, The Assam Royal Global University, Guwahati, Assam 781035, India
[2] School of Physics, Damghan University, P. O. Box 3671641167, Damghan, Iran
[3] Center for Theoretical Physics, Khazar University, 41 Mehseti Street, AZ1096 Baku, Azerbaijan
[4] Laboratory of Theoretical and Applied Physics, Echahid Cheikh Larbi Tebessi University, 12001 Tebessa, Algeria

Received: 27 August 2025 / Accepted: 4 October 2025

Abstract In this study, we explore the thermodynamic properties of a Schwarzschild black hole (BH) embedded in an anti-de Sitter (AdS) background, which is further coupled with a cloud of strings and surrounded by a quintessence-like fluid. Beginning with the formulation of BH mass in terms of the event horizon radius, we incorporate the concept of pressure as related to the AdS curvature radius within the framework of extended phase space thermodynamics. Using this setup, we derive key thermodynamic quantities, including the Gibbs free energy and internal energy, to characterize the energetic behavior of the BH system. To assess the stability of the BH, we compute the specific heat capacity and analyze how it is influenced by external parameters, such as the string cloud and the quintessence-like fluid. These geometric and matter fields are shown to significantly modify the thermal response of the BH. Furthermore, we examine the inversion temperature associated with the BH and highlight its distinction from the standard Hawking temperature, providing deeper insight into the phase structure. Additionally, we investigate the Joule-Thomson expansion process and demonstrate how the aforementioned parameters affect this thermodynamic phenomenon, showing important aspects of BH cooling and heating behavior in an extended thermodynamic context.

1 Introduction

Black hole (BH) thermodynamics has evolved into a central and insightful field of gravitational physics, illustrating our information between geometry, quantum theory, and statistical mechanics, with many important results illustrated in the literature [1–7]. Fundamental thermodynamic variables, including entropy and temperature, are intimately related to geometric properties such as the event horizon's area and the surface gravity. Semiclassical investigations reveal that the emission of Hawking radiation inherently drives BHs toward thermal instability, as the temperature rises with decreasing horizon size, initiating a runaway heating process. Over the years, extensive studies have been devoted to understanding various aspects of BH thermodynamics, among which the question of thermal stability remains crucial. This stability, reflecting the system's resilience to small perturbations in its thermodynamic parameter influence, is often tested through its phase structure, especially near critical point information, using a variety of theoretical frameworks [8]. One of the most widely adopted methods for assessing BH stability is the computation of specific heat (C_p) since a positive heat capacity signifies a thermodynamically stable configuration [9,10]. Also, specific heat (C_p) analysis serves as a powerful diagnostic tool for exploring phase transitions in BH systems, where the sign change or divergence of the heat capacity provides insight into the underlying critical behavior [10–14], showing and illustrating two principal types: transitions indicated by finite changes in heat capacity (C_v) and those marked by its divergence.

The AdS/CFT correspondence [15] has revitalized interest in the study of asymptotically Anti-de Sitter (AdS) BHs,

[a] e-mail: faizuddinahmed15@gmail.com (corresponding author)
[b] e-mails: saeed.noorigashti70@gmail.com; sn.gashti@du.ac.ir
[c] e-mail: b.pourhassan@du.ac.ir
[d] e-mail: abdelmalekbouzenada@gmail.com

Published online: 14 October 2025

largely because of their effectiveness in modeling strongly coupled thermal field theories on the AdS boundary. These BHs are significant not only from the holographic perspective but also due to their rich bulk thermodynamic structure, which exhibits a variety of phase transitions. A well-known example is the first-order Hawking–Page transition between thermal AdS radiation and Schwarzschild-AdS BHs [16]. When conserved charges are introduced, the thermodynamics of AdS BHs display behavior strikingly similar to that of a Van der Waals fluid [17]. This analogy becomes more precise within the framework of extended phase space thermodynamics [18], where the cosmological constant Λ is promoted to a thermodynamic variable, interpreted as pressure, and allowed to vary in the first law of BH thermodynamics: $\delta M = (T\,\delta S + V\,\delta P + \cdots)$, where V is the thermodynamic volume conjugate to P. This formalism enables the formulation of a BH equation of state, $P = P(V, T)$, which can be directly compared with that of a conventional fluid. For instance, the Van der Waals fluid is governed by the two-parameter equation of state $T = \left(P + \frac{a}{v^2}\right)(v - b)$, where $v = V/N$ denotes the specific volume per degree of freedom, with N representing the number of microscopic constituents. The parameters $a > 0$ and $b > 0$ respectively capture the effects of attractive interactions and the finite size of fluid molecules. Remarkably, the thermodynamics of charged and rotating AdS BHs qualitatively reproduce the features of the Van der Waals fluid, including a first-order small/large BH phase transition analogous to the liquid–gas transition. This transition terminates at a critical point characterized by classical mean-field critical exponents [19]. In both systems, the Gibb's free energy exhibits a characteristic swallowtail structure, signaling the presence of a first-order phase transition.

In the domain of BH thermodynamics, anti-de Sitter (AdS) BHs have received considerable attention due to their rich phase structures and deep analogies with conventional thermodynamic systems. A notable milestone in this field was the discovery of the Hawking–Page phase transition, which illustrates and defines a shift between a Schwarzschild-AdS BH and thermal AdS spacetime, which also plays a crucial role in the AdS/CFT correspondence [5]. Later, Chamblin et al. established a remarkable correspondence between the phase behavior of charged AdS BHs and that of a liquid–gas system in van der Waals fluids, particularly in the context of Reissner–Nordström-AdS (RN-AdS) BHs [20,21]. This connection was significantly deepened with the formulation of the extended phase space approach, where the cosmological constant is interpreted as a thermodynamic pressure, leading to the identification of P–V criticality [8]. Within this framework, other phenomena such as reentrant phase transitions [22,23] and the presence of a triple point [24] have been tested, illustrating the idea that AdS BH models can show behaviors analogous to ordinary thermodynamic systems. The breadth of developments in this subject is captured in recent reviews such as [25]. In this context, explain the cosmological constant properties, as illustrated this concepts in this study [26], offering a method for extracting mechanical work from BHs. Also, this study was further extended through its application to the rankine cycle, envisioning BHs as efficient cosmic-scale power plants [27]. Up to now, thermodynamic properties of AdS BHs have been widely studied in the literature (see, Refs. [28–39]).

Another important line of inquiry is the Joule–Thomson expansion, first tested for charged AdS BH models in [40], which investigated inversion curves and critical behavior, revealing both parallels and distinctions with van der Waals systems. This study was subsequently generalized to Kerr-AdS BHs [41], holographic superfluids [42], and quintessence-modified Reissner–Nordström-AdS BHs [43], expanding the thermodynamic understanding of BHs across diverse gravitational frameworks. One of the significant areas of research within the field of BH thermodynamics is the investigation of phase transitions. This topic involves employing a variety of analytical and computational methods to explore and characterize the different types of phase transitions that BHs can undergo. In recent years, particular attention has been directed towards the thermodynamic topology of BHs, which has emerged as a highly influential and insightful approach for examining the nature and properties of these phase transitions across diverse BH systems. This novel perspective has contributed substantially to advancing our understanding of BH thermodynamics and the underlying physical mechanisms driving such transitions. For a more study on thermodynamic topology, readers can see these references [44–53].

By incorporating the cosmological constant into the thermodynamic framework of BHs, it becomes possible to analyze these objects in an extended phase space, opening the way to study thermodynamic laws, the weak cosmic censorship conjecture, BH heat engines, and the Joule–Thomson (J–T) expansion process. The first detailed investigation of the J–T effect in charged AdS BHs was conducted in [40], where the process, analogous to the classical thermodynamic expansion of a gas from high to low pressure through a porous plug under constant enthalpy, was formulated in the gravitational context. Since this pioneering work, the method has been extended to a wide range of BH geometries, including d-dimensional charged AdS BHs [54], RN-AdS BHs in $f(R)$ gravity [55], AdS-BH with a global monopole [56], regular (Bardeen)-AdS BHs [57], charged AdS-BH in rainbow gravity [58], Hayward-AdS-BH [59], AdS-BH with momentum relaxation [60], Bardeen-AdS BH [61,62], Lovelock gravity BHs [63], charged Gauss–Bonnet AdS-BH [64], AdS-BH in quasitopological electromagnetism [65], charged Hayward-AdS BH in extended phase space [66], and Hayward-AdS

BH surrounded by fluid of strings [67], Hayward-AdS BHs in 4D Einstein–Gauss–Bonnet gravity [68].

Our study focuses on the comprehensive thermodynamic analysis of a Schwarzschild BH embedded in an AdS spacetime, which is further modified by the presence of a cloud of strings and a surrounding quintessence-like fluid. Within the framework of extended phase space thermodynamics, where the negative cosmological constant is reinterpreted as a thermodynamic pressure related to the AdS curvature radius, we start by formulating the BH mass as a function of the event horizon radius. In this case, this formulation enables us to derive and examine a range of fundamental thermodynamic quantities, including the Gibbs free energy, internal energy, and specific heat capacity, providing a detailed description of the energetic and stability properties of the system. Also, our results show and illustrate the combined effects of the string cloud parameter and the quintessence-like fluid introduce significant modifications to the BH's thermal behavior, altering its heat capacity profile and stability domains. Also, to further illustrate the phase structure, we compute the inversion temperature and compare it with the Hawking temperature, identifying distinct features that shed light on the role of external fields in BH thermodynamics. In addition, we investigate the Joule–Thomson expansion process, emphasizing how the interplay between the cloud of strings and the quintessence-like background affects the transition between heating and cooling regimes, as well as the location of the inversion curves. In this case, this extended thermodynamic perspective not only deepens our understanding of BH systems with additional matter fields but also shows the intricate ways in which geometric modifications and exotic fluids influence both local stability and global phase behavior.

The structure of this paper is organized as follows: in Sect. 1, we present the introduction to our study. Also, Sect. 2 is devoted to the thermodynamic properties of the considered BH configuration, where we derive key quantities and explore their dependence on the system's parameters. In this case, in Sect. 2.1, we investigate the stability of the BH by testing specific heat behavior and related thermodynamic criteria. Another important result, Sect. 3 focuses on the thermodynamic geometry, employing geometric methods to illustrate the phase structures and BH parameter interactions. In this context, in Sect. 4, we determine the inversion temperature, which marks the transition between cooling and heating phases under the Joule–Thomson process. The next Sect. 5, is a detailed discussion of the Joule–Thomson expansion, where we analyze the isenthalpic curves and the corresponding physical implications. Finally, Sect. 6 shows the main findings, illustrates the significance of the results, and suggests possible directions for future research.

2 Thermodynamics of AdS BH with CoS and QF

In this section, we explore the thermodynamic properties of an AdS BH model coupled to a cloud of strings and surrounded by a quintessence-like fluid. We derive the corresponding thermodynamic quantities-such as the Hawking temperature, Gibbs free energy, internal energy, and specific heat capacity and examine how the presence of CoS and QF affects these variables. In this framework, the BH mass is interpreted as the enthalpy, the event horizon area as the entropy [69], and the cosmological constant is identified with the thermodynamic pressure in extended phase space formalism [5,8].

The first spherically symmetric BH solution incorporating a cloud of strings was proposed by Letelier [70], where the cloud arises from an electric-like component. This configuration modifies the horizon structure of the BH, leading to an event horizon radius given by $r_h = \frac{2M}{1-\alpha}$, where α denotes the string parameter. This expression indicates a deviation from the standard Schwarzschild radius $r_{\rm Sch} = 2M$, implying that the presence of the string cloud enlarges the event horizon ($r_h > r_{\rm Sch}$). Furthermore, the spacetime exhibits a solid angle deficit, similar to the geometry associated with a global monopole [71]. These modifications suggest potentially significant astrophysical consequences, thereby motivating further investigations into BHs surrounded by string clouds. More recently, the original model by Letelier [70] has been generalized by incorporating a magnetic-like component alongside the electric-like one, as discussed in [72]. The combined presence of these components leads to further modifications of the horizon radius and alters the overall space-time geometry in a more complex manner.

On another front, the discovery of the accelerated expansion of the universe stands as one of the most remarkable achievements in observational cosmology [73–75]. This phenomenon implies the existence of a gravitationally repulsive component with negative pressure, commonly referred to as dark energy. A widely studied model of dark energy is quintessence, which is modeled as a spatially homogeneous, time-independent fluid. Its pressure p_q is proportional to its energy density ρ_q, with the equation-of-state parameter ω_q defined as, $w_q = p_q/\rho_q$. In this context, Kiselev's solution to the Einstein field equations, which describes a BH surrounded by quintessence-like fluid, provides important insights into how such exotic energy components influence the structure and properties of BHs [76]. In order to obtain a cosmological horizon similar to the Schwarzschild-de Sitter BH, the state parameter lying in the range $-1 < \omega < -1/3$. The special case $\omega = -1$ corresponds to the cosmological constant, often considered the simplest form of dark energy. Quintessence plays a significant role in explaining cosmic acceleration and has inspired various theoretical frameworks.

Motivated by the above works, the present study considers a spherically symmetric AdS BH solution influenced by two significant external sources: a generalized form of cloud of strings and quintessence-like field. We investigate how these factors modify the thermodynamic properties of the BH system. Thereby, a static and spherically symmetric AdS BH space-time with a CoS and surrounded by a QF is described by the following line element [77,78]

$$ds^2 = -f(r)\,dt^2 + \frac{1}{f(r)}\,dr^2 + r^2\,(d\theta^2 + \sin^2\theta d\phi^2), \quad (1)$$

with the metric function is given by

$$f(r) = 1 - \frac{2\,M}{r} + \frac{|\alpha|\,b^2}{r^2}\,{}_2F_1\left(-\frac{1}{2}, -\frac{1}{4}, \frac{3}{4}, -\frac{r^4}{b^4}\right) - \frac{\mathrm{N}}{r^{3\,w+1}} + \frac{r^2}{\ell_p^2} \quad (-1 < w < -1/3), \quad (2)$$

Here $(|\alpha|, b)$ represents the CoS parameters [70,72] and (N, w) denotes the QF parameters [79]. The quintessence parameter $\omega = p/\rho$ characterizes the equation of state of dark energy and governs its repulsive effect driving cosmic acceleration. In BH spacetimes, ω determines the surrounding fluid's density profile, influencing the metric, thermodynamic properties, and phase transitions. Observational constraints on ω from supernovae, CMB, and large-scale structure guide its allowed range in these models. Variations in ω affect BH stability, evaporation, and cosmological implications, linking local astrophysical phenomena to global dynamics. Thus, ω provides a bridge between BH physics and dark energy cosmology [80].

In the limit $b \to 0$, the hypergeometric term in the metric function behaves as

$$\lim_{b\to 0} \frac{|\alpha|\,b^2}{r^2}\,{}_2F_1\left(-\frac{1}{2}, -\frac{1}{4}; \frac{3}{4}; -\frac{r^4}{b^4}\right) \approx -|\alpha|. \quad (3)$$

By setting $|\alpha| = \alpha$, the metric function $f(r)$ given in Eq. (2) in the limit $b \to 0$ reduces to

$$f(r) = 1 - \alpha - \frac{2M}{r} - \frac{\mathrm{N}}{r^{3w+1}} + \frac{r^2}{\ell_p^2}, \quad (4)$$

which corresponds to the Letelier-AdS BH solution surrounded by a quintessence-like fluid, as discussed in [81].

Let us now proceed to study this process for the BH. First of all, let us compute the BH mass M, which is defined as a function of the location of its horizon r_+, through the largest root of $f(r = r_+) = 0$, before any cosmological horizon. Then by using Eq. (2), one gets

$$M = \frac{r_+}{2}\left[1 + \frac{|\alpha|\,b^2}{r_+^2}\,{}_2F_1\left(-\frac{1}{2}, -\frac{1}{4}, \frac{3}{4}, -\frac{r_+^4}{b^4}\right) - \frac{\mathrm{N}}{r_+^{3\,w+1}} + \frac{8\pi}{3}\,P\,r_+^2\right], \quad (5)$$

with M interpreted as the enthalpy of the system and we have used the thermodynamic pressure in extended phase space of the following form [8]:

$$P = \frac{3}{8\,\pi\,\ell_p^2}. \quad (6)$$

In Fig. 1, we present the BH mass M as a function of the horizon radius r_+, while varying the CoS parameter α and the state parameter w of QF. In both panels, it is evident that increasing either α or w causes an upward shift in the mass curve. This indicates that stronger coupling through the CoS parameter or a stiffer QF (higher w) leads to a larger BH mass for the same horizon radius. Thus, the interplay between α and w significantly affects the BH mass spectrum, reflecting their impact on the spacetime geometry and matter distribution around the BH.

The thermodynamic volume V can be determined using the following relation:

$$V = \frac{\partial M}{\partial P} = \frac{4\pi}{3}\,r_+^3. \quad (7)$$

The Hawking temperature is given by

$$T = \frac{f'(r_+)}{4\pi} = \frac{1}{4\pi\,r_+}\left[1 - |\alpha|\,b^2\left\{\frac{1}{r_+^2}\,{}_2F_1\left(-\tfrac{1}{2}, -\tfrac{1}{4}, \tfrac{3}{4}, -\tfrac{r_+^4}{b^4}\right) + \frac{2\,r_+^2}{3\,b^4}\,{}_2F_1\left(\tfrac{1}{2}, \tfrac{3}{4}, \tfrac{7}{4}, -\tfrac{r_+^4}{b^4}\right)\right\} + 3\,w\,\mathrm{N}\,r_+^{-3w-2} + 8\,\pi\,P\,r_+^2\right]. \quad (8)$$

From expression (8), it becomes evident that the Hawking temperature is influenced by the parameters of CoS, namely $(\alpha,\ b)$, the QF parameters $(\mathrm{N},\ w)$, as well as the thermodynamic pressure P.

In the limiting case where $b \to 0$, and $|\alpha| = \alpha$, the Hawking temperature obtained in Eq. (8) reduces to the expression previously reported in [81]. This confirms that the additional CoS parameter b introduces a non-trivial modification to the known temperature, effectively shifting the result due to the extended structure of the string cloud.

Figure 2 illustrates the behavior of the Hawking temperature T_H as a function of the horizon radius r_+, with variations in the CoS parameter α and the state parameter w of QF. In panel (i), we observe that increasing the value of α leads to a decrease in the Hawking temperature. This suggests that stronger contributions from the CoS sector shift the BH toward a cooler thermodynamic regime. In contrast, panel (ii) shows that as the state parameter w increases-corresponding to a stiffer QF-the Hawking temperature rises. This indicates that a more rigid QF environment tends to heat the

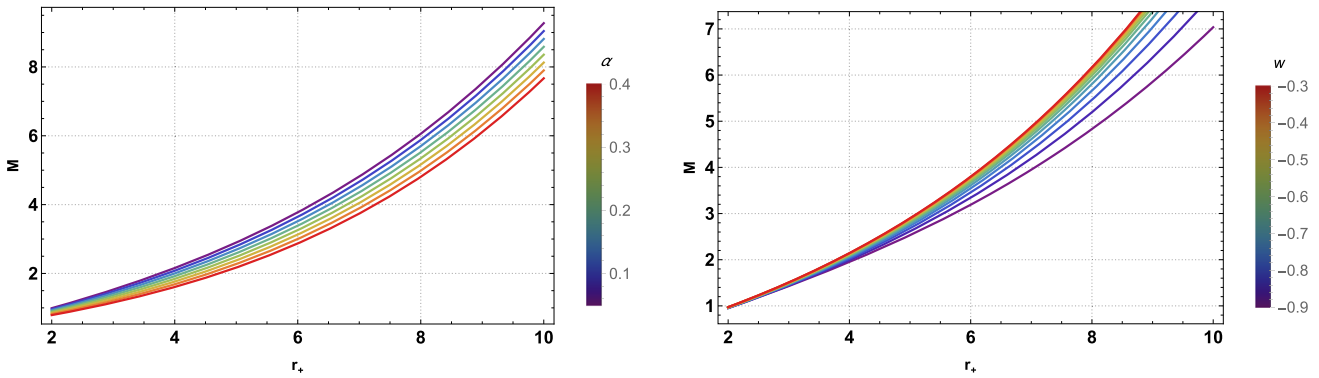

(i) $w = -2/3$ (ii) $\alpha = 0.1$

Fig. 1 Behavior of the BH mass M as a function of horizon for different values of CoS parameter α and state parameter W. Here $\mathrm{N} = 0.01,\ b = 0.5,\ \ell_p = 10$

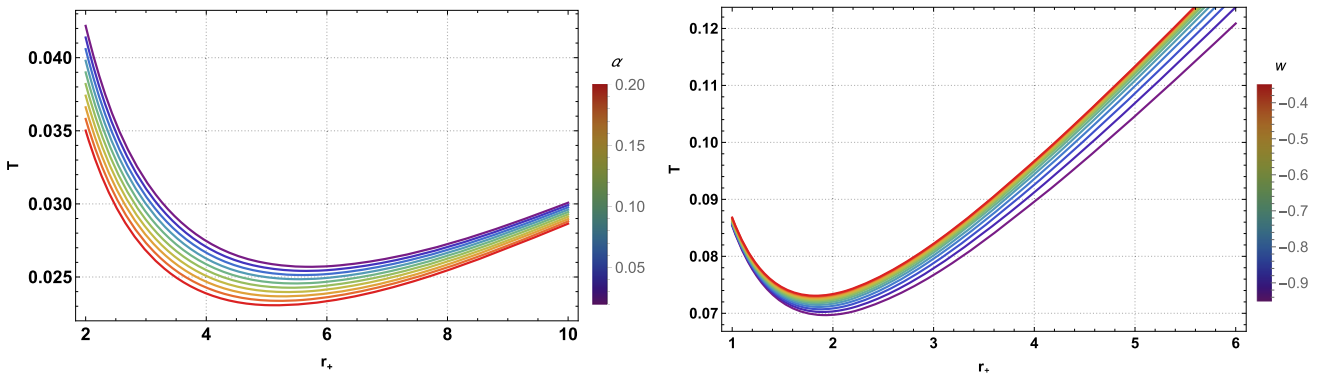

(i) $w = -2/3$ (ii) $\alpha = 0.15$

Fig. 2 Behavior of the Hawking temperature T given in Eq. (8) as a function of horizon for different values of CoS parameter α and state parameter W. Here $b = 0.1,\ w = -2/3,\ \mathrm{N} = 0.01,\ P = 0.01$

BH. Together, these observations show that the parameters α and w play competing roles in the thermal behavior of the BH: while α tends to suppress the temperature, w enhances it. Their interplay therefore crucially influences the thermodynamic phase space of the system.

We can more prominently analyze the behavior of the Gibbs free energy, F, of this BH, as it provides valuable insights into the thermodynamic processes occurring within the BH system, particularly those related to phase transitions and critical phenomena. The Gibbs free energy, a fundamental thermodynamic potential, is defined by the relation;

$$F = M - T\,S, \tag{9}$$

where M denotes the mass (or internal energy) of the BH, T represents its Hawking temperature, and S is the entropy associated with the BH horizon.

To compute the entropy of the BH, one can see in Ref. [82] that this entropy is the same as Hawking–Bekenstein entropy, so that

$$S = \pi\, r_+^2. \tag{10}$$

This definition encapsulates the balance between the energy content and thermal effects of the BH system, making F a crucial quantity for studying its stability and phase behavior. By substituting the explicit expressions for M, T, and S, as previously derived in Eqs. (5), (8), and (10) respectively, one can obtain an explicit analytical form for the Gibbs free energy:

$$\begin{aligned} F = {} & \frac{1}{4} r_+ + \frac{|\alpha|\, b^2}{4\, r_+}\, {}_2F_1\left(-\tfrac{1}{2}, -\tfrac{1}{4}, \tfrac{3}{4}, -\tfrac{r_+^4}{b^4}\right) \\ & - \frac{|\alpha|\, r_+^3}{6\, b^2}\, {}_2F_1\left(\tfrac{1}{2}, \tfrac{3}{4}, \tfrac{7}{4}, -\tfrac{r_+^4}{b^4}\right) \\ & - \left(\frac{2+3w}{4}\right) \frac{\mathrm{N}}{r_+^{3w}} - \frac{2\,\pi}{3}\, P\, r_+^3 \end{aligned} \tag{11}$$

From expression (11), it becomes evident that the Gibb's free energy is influenced by the CoS parameters (α, b), the QF parameters (N, w), and the thermodynamic pressure P.

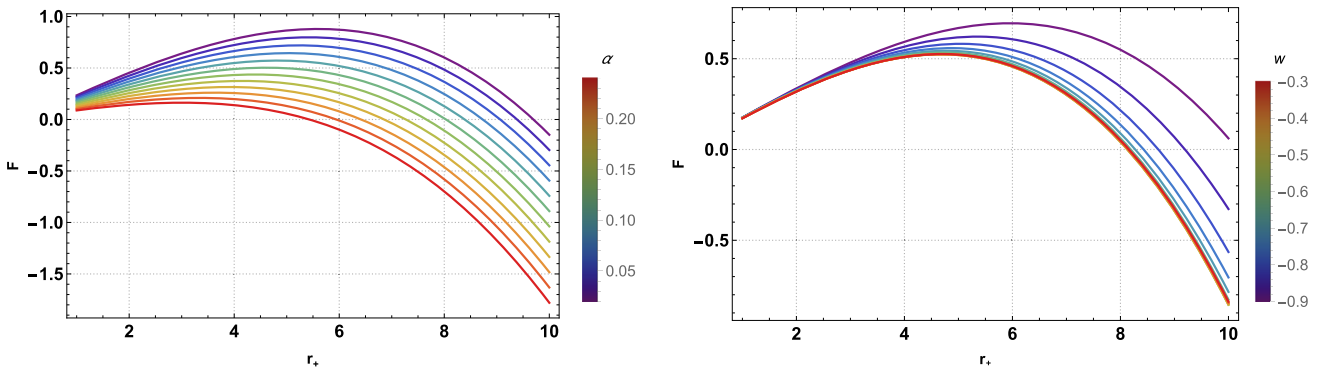

(i) $w = -2/3$ (ii) $\alpha = 0.1$

Fig. 3 Behavior of the Gibb's free energy F given in Eq. (11) as a function of horizon for different values of CoS parameter α and state parameter W. Here, N = 0.01, $\ell_p = 10$, $b = 0.1$

In the limiting case where $b \to 0$, and $|\alpha| = \alpha$, the Gibb's free energy obtained in Eq. (11) reduces to the expression previously reported in [81]. This confirms that the additional CoS parameter b introduces a modification to the known free energy, effectively shifting the result due to the extended structure of the string cloud.

Finally, the internal energy of the system is given by

$$U = M - P\,V = \frac{r_+}{2}\left[1 + \frac{|\alpha|\,b^2}{r_+^2}\,{}_2F_1 \times \left(-\frac{1}{2}, -\frac{1}{4}, \frac{3}{4}, -\frac{r_+^4}{b^4}\right) - \frac{\mathrm{N}}{r_+^{3\,w+1}}\right]. \tag{12}$$

From expression (12), it becomes evident that the internal energy of the thermodynamic system is influenced by the CoS parameters (α, b), the QF parameters (N, w), as well as the thermodynamic pressure P.

In the limiting case where $b \to 0$ and $|\alpha| = \alpha$, the internal energy simplifies to $U = \frac{r_+}{2}\left(1 - \alpha - \frac{\mathrm{N}}{r_+^{3w+1}}\right)$, which coincides with the expression obtained from the metric presented in [81]. This agreement confirms that the additional cloud of strings (CoS) parameter b introduces a non-trivial modification to the internal energy, effectively shifting the known result due to the extended structure associated with the string cloud.

Equation (11) explicitly relates F to the horizon radius r_+ and other relevant parameters of the BH, enabling a detailed analysis of its thermodynamic properties. Figure 3 presents the variation of the free energy F as a function of the horizon radius r_+. From this plot, it is evident that the free energy exhibits distinct features at r_+. These features signify the occurrence of phase transitions, indicating changes in the stability and configuration of the BH states. The behavior of F with respect to r_+ thus serves as a powerful diagnostic tool for understanding the thermodynamic phase structure of the BHs under consideration. In particular, the presence of multiple branches or turning points in the F versus r_+ curve suggests rich thermodynamic phenomena, such as first-order or second-order phase transitions, and critical points. Such phenomena are essential for comprehending the microphysical processes governing BH thermodynamics and can shed light on the interplay between gravity, quantum effects, and thermodynamics in these extreme systems.

Furthermore, as illustrated in Fig. 4, we analyze the behavior of the internal energy U, as defined in Eq. (12), plotted as a function of the BH horizon radius. This analysis is carried out for various values of the coefficient of state (CoS) parameter α as well as different values of the equation of state parameter ω. The figure clearly demonstrates how changes in these parameters influence the thermodynamic behavior of the system, particularly highlighting the sensitivity of the internal energy to both the gravitational modifications introduced by α and the matter content encoded in ω. Such dependencies offer deeper insight into the interplay between geometry and matter in modified gravity scenarios and can shed light on the underlying microphysics near BH horizons.

2.1 Specific heat capacity: stability of BH

To comprehensively understand the thermodynamic behavior and stability characteristics of the Schwarzschild-AdS BHs with cloud of strings and quintessential-like fluid, we analyze its specific heat at constant parameters. This quantity provides critical insights into the response of the system to thermal fluctuations and serves as an indicator of local thermodynamic stability. The specific heat is derived using the expressions for the Hawking temperature T, given in Eq. (8), and the entropy S, given in Eq. (10). Employing the fundamental thermodynamic iden-

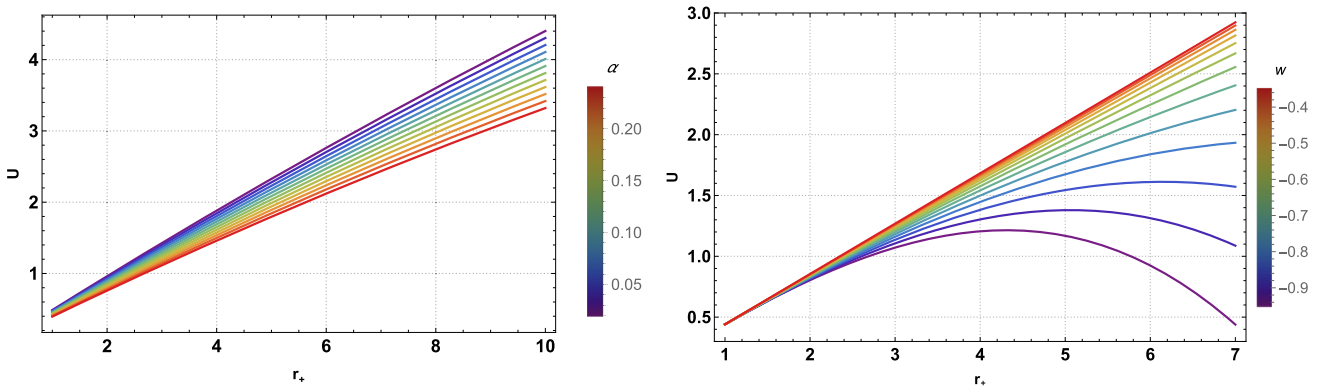

(i) $w = -2/3$ (ii) $\alpha = 0.1$

Fig. 4 Behavior of the internal energy U given in Eq. (12) as a function of horizon for different values of CoS parameter α and state parameter W. Here $b = 0.2,\ \mathrm{N} = 0.01$

tity, the specific heat at constant parameters is defined as [8,83]:

$$C_p = T\left(\frac{\partial S}{\partial T}\right) = T\left(\frac{\partial S}{\partial r_+}\right)\left(\frac{\partial T}{\partial r_+}\right)^{-1}, \tag{13}$$

Using the Hawking temperature given in Eq. (8) and the entropy in Eq. (10), the specific heat capacity simplifies to

$$C_p = \frac{2\pi r_+^2\left[\frac{1}{r_+^2} - \frac{|\alpha|b^2}{r_+}\left\{\frac{1}{r_+^3}\,{}_2F_1\left(-\frac{1}{2},-\frac{1}{4},\frac{3}{4},-\frac{r_+^4}{b^4}\right) + \frac{2}{3b^4}\,{}_2F_1\left(\frac{1}{2},\frac{3}{4},\frac{7}{4},-\frac{r_+^4}{b^4}\right)\right\} + 3\,w\,\mathrm{N}\,r_+^{-3w-3} + 8\pi P\right]}{\left[-\frac{1}{r_+^2} + |\alpha|b^2\left\{\frac{3}{r_+^4}\,{}_2F_1\left(-\frac{1}{2},-\frac{1}{4},\frac{3}{4},-\frac{r_+^4}{b^4}\right) + \frac{2}{3b^4}\,{}_2F_1\left(\frac{1}{2},\frac{3}{4},\frac{7}{4},-\frac{r_+^4}{b^4}\right) - \frac{6,r_+^3}{7b^8}\,{}_2F_1\left(\frac{3}{2},\frac{7}{4},\frac{11}{4},-\frac{r_+^4}{b^4}\right)\right\} - \frac{3w\,\mathrm{N}(3w+2)}{r_+^{3w+3}} + 8\pi P\right]} \tag{14}$$

From expression (14), it becomes evident that the specific heat capacity is influenced by the CoS parameters (α, b) and the QF parameters (N, w), as well as the thermodynamic pressure including the horizon.

In the limiting case $b \to 0$ and $|\alpha| = \alpha$, the specific heat capacity reduces to the following form:

$$C_p = \frac{2\pi r_+^2\left[1 - \alpha + \frac{3w\mathrm{N}}{r_+^{3w+2}} + 8\pi P\right]}{-1 + \alpha - \frac{3w\mathrm{N}(3w+2)}{r_+^{3w+1}} + 8\pi P\, r_+^2}. \tag{15}$$

This expression clearly shows that the parameter α, associated with the cloud of strings, remains present and continues to influence the thermodynamic behavior even in the $b \to 0$ limit. From the above analysis, it confirms that the additional CoS parameter b introduces a non-trivial modification to the specific heat capacity C_p given in Eq. (14), effectively shifting the known result due to the extended structure associated with the string cloud.

For a particular state parameter, $w = -2/3$, the specific heat reduces given in Eq. (14) reduces as,

$$C_p = \frac{2\pi r_+^2\left[\frac{1}{r_+^2} - \frac{|\alpha|b^2}{r_+}\left\{\frac{1}{r_+^3}\,{}_2F_1\left(-\frac{1}{2},-\frac{1}{4},\frac{3}{4},-\frac{r_+^4}{b^4}\right) + \frac{2}{3b^4}\,{}_2F_1\left(\frac{1}{2},\frac{3}{4},\frac{7}{4},-\frac{r_+^4}{b^4}\right)\right\} - \frac{2\mathrm{N}}{r_+} + 8\pi P\right]}{\left[-\frac{1}{r_+^2} + |\alpha|b^2\left\{\frac{3}{r_+^4}\,{}_2F_1\left(-\frac{1}{2},-\frac{1}{4},\frac{3}{4},-\frac{r_+^4}{b^4}\right) + \frac{2}{3b^4}\,{}_2F_1\left(\frac{1}{2},\frac{3}{4},\frac{7}{4},-\frac{r_+^4}{b^4}\right) - \frac{6r_+^3}{7b^8}\,{}_2F_1\left(\frac{3}{2},\frac{7}{4},\frac{11}{4},-\frac{r_+^4}{b^4}\right)\right\} + 8\pi P\right]} \tag{16}$$

The analysis of the specific heat not only identifies the conditions under which the BH undergoes phase transitions but also provides a consistent thermodynamic interpretation of stability properties inferred from topological methods. The interplay between thermal stability and topological characteristics underscores the robustness of the thermodynamic framework in exploring modified gravity scenarios.

The behavior of C_p as a function of the BH parameters reveals several notable features that determine in Fig. 5:

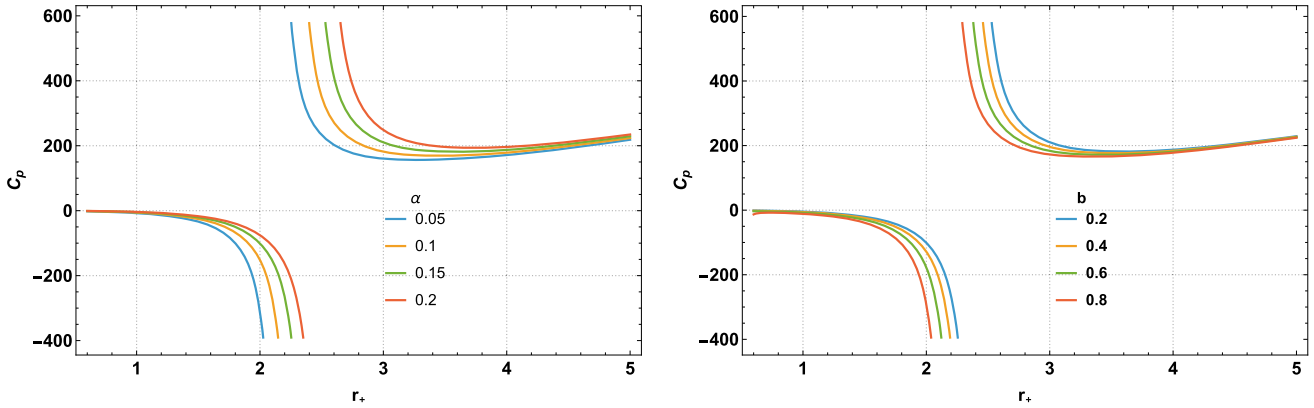

(i) $b = 0.2$ (ii) $\alpha = 0.1$

Fig. 5 Behavior of the specific heat capacity C_p given in Eq. (16) as a function of horizon for different values of CoS parameters α and b. Here, we set $w = -2/3,\ \mathrm{N} = 0.01,\ P = 0.01$

- *Phase transitions:* The specific heat diverges at certain critical values of the horizon radius or other control parameters. These divergences signal second-order phase transitions, marking qualitative changes in the thermodynamic structure of the BH.
- *Thermal stability:* In regions where the specific heat is positive ($C_p > 0$), the BH exhibits thermal stability, indicating that it can maintain equilibrium under small perturbations. Conversely, negative specific heat ($C_p < 0$) corresponds to thermal instability, a characteristic feature of many BH systems. The analysis of the specific heat not only identifies the conditions under which the BH undergoes phase transitions but also provides a consistent thermodynamic interpretation of stability properties inferred from topological methods. The interplay between thermal stability and topological characteristics underscores the robustness of the thermodynamic framework in exploring modified gravity scenarios.

3 Thermodynamic geometry of AdS BH with CoS and QF

In addition to the standard thermodynamic stability analysis, it is instructive to examine the Schwarzschild–AdS BH with a cloud of strings and quintessential-like fluid from the perspective of thermodynamic geometry. This approach, known as geometrothermodynamics [84,85], equips the space of equilibrium states with a Riemannian metric whose curvature encodes information about the microscopic interactions underlying the thermodynamic system [86,87]. In this framework, we adopt the Ruppeiner metric, which is defined in the entropy representation as,

$$g^R_{ij} = -\frac{\partial^2 S}{\partial X^i \partial X^j}, \tag{17}$$

where X^i are the extensive variables of the system. Equivalently, the Ruppeiner metric is conformally related to the Weinhold metric via $g^R_{ij} = \frac{1}{T} g^W_{ij}$, with

$$g^W_{ij} = \frac{\partial^2 M}{\partial X^i \partial X^j}. \tag{18}$$

For our BH configuration, we choose the thermodynamic coordinates $X^i = (S, P)$ while holding $(|\alpha|, b, N, w)$ fixed. Using Eq. (5), the Weinhold metric components are

$$g^W_{SS} = \frac{\partial^2 M}{\partial S^2}, \tag{19}$$

$$g^W_{SP} = \frac{\partial^2 M}{\partial S \partial P} = g^W_{PS}, \tag{20}$$

$$g^W_{PP} = \frac{\partial^2 M}{\partial P^2}, \tag{21}$$

where

$$M(S,P) = \frac{\sqrt{\pi}}{2}\left[\sqrt{S} + \frac{\pi|\alpha|b^2\sqrt{S}}{2F_1\left(-\frac{1}{2}, -\frac{1}{4}; \frac{3}{4}; -\frac{S^2}{\pi^2 b^4}\right)} - N S^{-\frac{3w}{2}} \pi^{\frac{3w+1}{2}} + \frac{8P}{3} S^{3/2}\right], \tag{22}$$

The Ruppeiner curvature scalar R_R, obtained from the thermodynamic metric g^R_{ij}, encodes valuable information about the microscopic interactions of the system. A positive value of R_R corresponds to predominantly repulsive interactions between the hypothetical microscopic constituents of the BH, whereas a negative value signals the dominance of attractive interactions. When R_R diverges, it typically marks the location of a phase transition, coinciding with points where other thermodynamic quantities such as the specific heat also become singular. Thus, the sign and divergence

structure of R_R provide a geometric probe of the BH's thermodynamic stability and microphysical behavior. By explicitly computing R_R for various values of (α, b, N, w), we find,

$$R_R(S,P)=\frac{-\frac{\sqrt{\pi}}{8}S^{-5/2}+\frac{3w(3w+2)}{8}N\pi^{\frac{3w+1}{2}}S^{-\frac{3w}{2}-2}}{\frac{32\pi}{9}T(S,P)\,S} +\frac{9\sqrt{\pi}|\alpha|b^2\left[\frac{15}{8}S^{-7/2}\,{}_2F_1\left(-\frac{1}{2},-\frac{1}{4};\frac{3}{4};-\frac{S^2}{\pi^2b^4}\right)+\frac{5S^{-3/2}}{3\pi^2b^4}\,{}_2F_1\left(\frac{1}{2},\frac{3}{4};\frac{7}{4};-\frac{S^2}{\pi^2b^4}\right)+\frac{2S^{1/2}}{9\pi^4b^8}\,{}_2F_1\left(\frac{3}{2},\frac{7}{4};\frac{11}{4};-\frac{S^2}{\pi^2b^4}\right)\right]}{64\,T(S,P)\,S}. \quad (23)$$

where

$$T(S,P)=\frac{1}{4\sqrt{\pi}}\left[\frac{1}{\sqrt{S}}-\pi|\alpha|b^2\left\{\frac{1}{S^{3/2}}\,{}_2F_1\left(-\frac{1}{2},-\frac{1}{4};\frac{3}{4};-\frac{S^2}{\pi^2b^4}\right)+\frac{2\sqrt{S}}{3\pi^2b^4}\,{}_2F_1\left(\frac{1}{2},\frac{3}{4};\frac{7}{4};-\frac{S^2}{\pi^2b^4}\right)\right\}+3wNS^{-\frac{3w}{2}-1}\pi^{\frac{3w+1}{2}}+8P\sqrt{S}\right]. \quad (24)$$

The analysis reveals that the Ruppeiner curvature scalar diverges exactly at the points where the specific heat changes sign, thereby confirming the close correspondence between the geometric description of the thermodynamic state space and the conventional stability analysis. Away from these critical points, both the sign and the magnitude of R_R are found to be strongly affected by the cloud of strings parameter α and the quintessential-like fluid parameter N, demonstrating that these external fields have a direct impact on the effective microscopic interactions of the BH. Furthermore, in the regime of large horizon radii, or equivalently large entropy S, the curvature scalar approaches zero, indicating that the microscopic structure of the BH tends toward an ideal-gas-like behavior in this limit (see Fig. 6).

This geometric perspective thus reinforces the phase structure obtained earlier and offers an interpretation in terms of underlying microphysical interactions. Moreover, it highlights how external matter fields such as a cloud of strings and quintessence-like fluid can imprint distinct geometric signatures in the thermodynamic state space of the BH.

4 Inversion temperature of AdS BH with CoS and QF

The BH mass M in Eq. (5) can be expressed in terms of the entropy of the BH whose relation to the area of the horizon A is given by $S = A/4 = \pi r_+^2$. Thus, in terms of entropy, Eq. (5) simplifies to

$$M=\frac{1}{2\sqrt{\pi}}\left[\sqrt{S}+\frac{\pi\,|\alpha|\,b^2}{\sqrt{S}}\,{}_2F_1\left(-\frac{1}{2},-\frac{1}{4},\frac{3}{4},-\frac{S^2}{\pi^2\,b^4}\right)-\mathrm{N}\,S^{-3\,w/2}\,\pi^{(3\,w+1)/2}+\frac{8}{3}\,P\,S^{3/2}\right]. \quad (25)$$

In Fig. 7, we investigate the behavior of the BH mass M, as defined in Eq. (22), by plotting it as a function of the entropy. This analysis is conducted for various values of the (CoS) parameter α and the equation of state parameter ω, while keeping the parameters $\mathrm{N} = 0.01$ and $P = 0.01$ fixed throughout. The figure illustrates how modifications in α and ω influence the thermodynamic mass of the BH, thereby offering valuable insight into how these parameters affect the underlying gravitational and thermodynamic structure of the system. Specifically, variations in α reflect the influence of the modified gravity framework, whereas changes in ω encode the effects of different types of matter or energy content. This analysis highlights the intricate dependence of BH mass on entropy under nontrivial thermodynamic and gravitational corrections, which is essential for a deeper understanding of BH microphysics in extended theories of gravity.

The BH mass of Eq. (25) can be written as $M = M(S, P, |\alpha|, b, \mathrm{N})$. Considering the parameters related to the cloud of strings and the quintessence, respectively $(|\alpha|, b)$ and N, are extensive thermodynamic parameters. As a consequence , the first law of BH thermodynamics must be modified to

$$dM = T_H\,dS + V\,dP + \mathcal{A}_H\,d|\alpha| + \mathcal{B}_H\,db + \mathcal{C}_H\,d\mathrm{N}, \quad (26)$$

where $\mathcal{A}$ and $\mathcal{B}$ are the intensive thermodynamic variables conjugate to the CoS parameters $(|\alpha|, b)$ and $\mathcal{C}$ is another intensive variables related to the normalization constant N of QF. Moreover T is the temperature, V is the volume of the BH. All these variables can be calculated as,

$$T_H=\left(\frac{\partial M}{\partial S}\right)_{P,|\alpha|,b,\mathrm{N}}, \quad (27)$$

$$V=\left(\frac{\partial M}{\partial P}\right)_{S,|\alpha|,b,\mathrm{N}}=\frac{4}{3}\,S\,\sqrt{S/\pi}, \quad (28)$$

$$\mathcal{A}_H=\left(\frac{\partial M}{\partial|\alpha|}\right)_{S,P,b,\mathrm{N}}=\frac{b^2}{2}\sqrt{\frac{\pi}{S}}\,{}_2F_1\left(-\frac{1}{2},-\frac{1}{4},\frac{3}{4},-\frac{S^2}{\pi^2\,b^4}\right), \quad (29)$$

$$\mathcal{B}_H=\left(\frac{\partial M}{\partial b}\right)_{S,P\,|\alpha|,\mathrm{N}}=\sqrt{\pi/S}\,|\alpha| \times\left[b\,{}_2F_1\left(-\frac{1}{2},-\frac{1}{4},\frac{3}{4},-\frac{S^2}{\pi^2\,b^4}\right)+\frac{S^2}{3\,\pi^2\,b^3}\,{}_2F_1\left(\frac{1}{2},\frac{3}{4};\frac{7}{4};-\frac{S^2}{\pi^2\,b^4}\right)\right], \quad (30)$$

$$\mathcal{C}_H=\left(\frac{\partial M}{\partial \mathrm{N}}\right)_{S,P,|\alpha|,b}=-\frac{1}{2}\,S^{-3\,w/2}\,\pi^{3\,w/2}=-\frac{1}{2}\,(\pi/S)^{3w/2}. \quad (31)$$

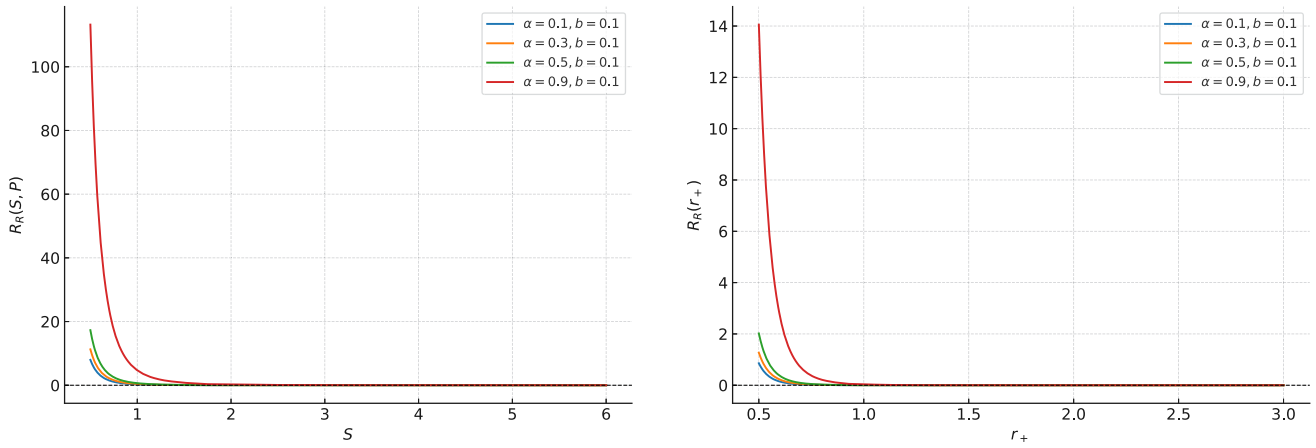

Fig. 6 Ruppeiner curvature scalar R_R as a function of entropy S for different values of α and fixed parameters $b = 0.1$, $N = 0.02$, $\omega = -2/3$, and $P = 0.001$. The divergence points correspond to phase transitions identified via the specific heat analysis

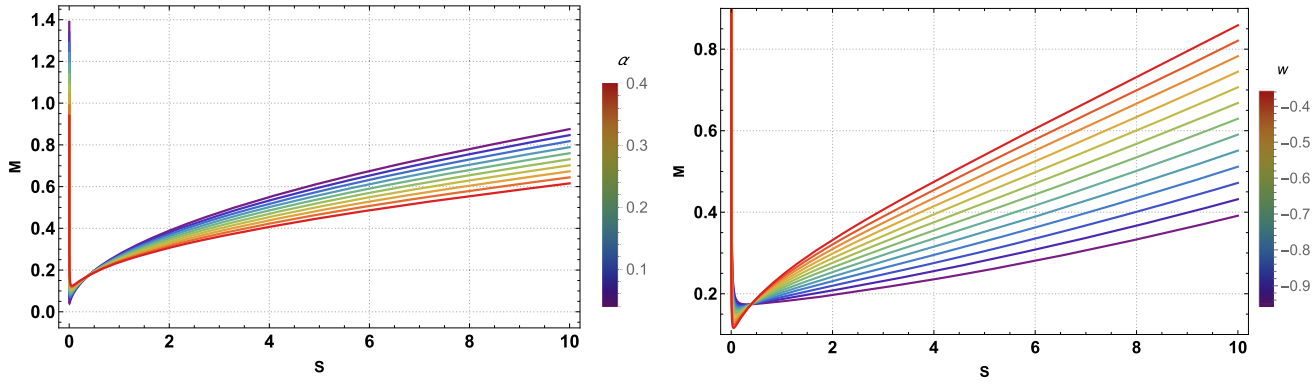

(i) $w = -2/3$ (ii) $\alpha = 0.15$

Fig. 7 Behavior of the BH mass M given in Eq. (25) as a function of entropy for different values of CoS parameter α and state parameter w. Here, we set N = 0.01, $b = 0.2$, $ell_p = 10$

In Fig. 8, we examine the behavior of the intensive thermodynamic variables A_H and B_H as functions of the entropy S, for various values of the (CoS) parameter b. This analysis allows us to explore how changes in the parameter b, which encapsulates the deviation from standard thermodynamic behavior due to modifications in the underlying gravitational theory or matter content, affect the intensive properties of the BH system. The figure reveals that both A_H and B_H exhibit distinct and sensitive responses to variations in entropy depending on the chosen value of b, indicating that the thermodynamic phase structure is deeply influenced by the specific CoS regime considered. Such an investigation provides a deeper understanding of how intensive variables evolve in extended thermodynamic settings and offers important clues about the microphysical interpretation of BH thermodynamics in modified gravity scenarios.

Let us now calculate the temperature T_H using Eq. (25). By definition in Eq. (27), we find the temperature as,

$$T_H = \frac{1}{4\sqrt{\pi\, S}}\Bigg[1 - |\alpha|\, b^2 \left\{\frac{\pi}{S}\, {}_2F_1\left(-\tfrac{1}{2}, -\tfrac{1}{4}, \tfrac{3}{4}, -\frac{S^2}{\pi^2 b^4}\right) + \frac{2\,S}{3\,\pi\, b^4}\, {}_2F_1\left(\tfrac{1}{2}, \tfrac{3}{4}, \tfrac{7}{4}, -\frac{S^2}{\pi^2 b^4}\right)\right\} + 3\, w\, \mathrm{N}\, (\pi/S)^{\frac{3w+1}{2}} + 8\, P\, S\Bigg]. \tag{32}$$

We can see that the temperature T_H when express in terms of horizon is the same expression as the Hawking temperature T obtained in Eq. (8).

In Fig. 9, we analyze the behavior of the Hawking temperature T_H, as defined in Eq. (29), plotted as a function of the entropy S for different values of CoS parameter α and the equation-of-state (EoS) parameter ω. For clarity and to isolate the role of these parameters, the constants $N = 0.01$ and $P = 0.01$ are kept fixed throughout the analysis. This

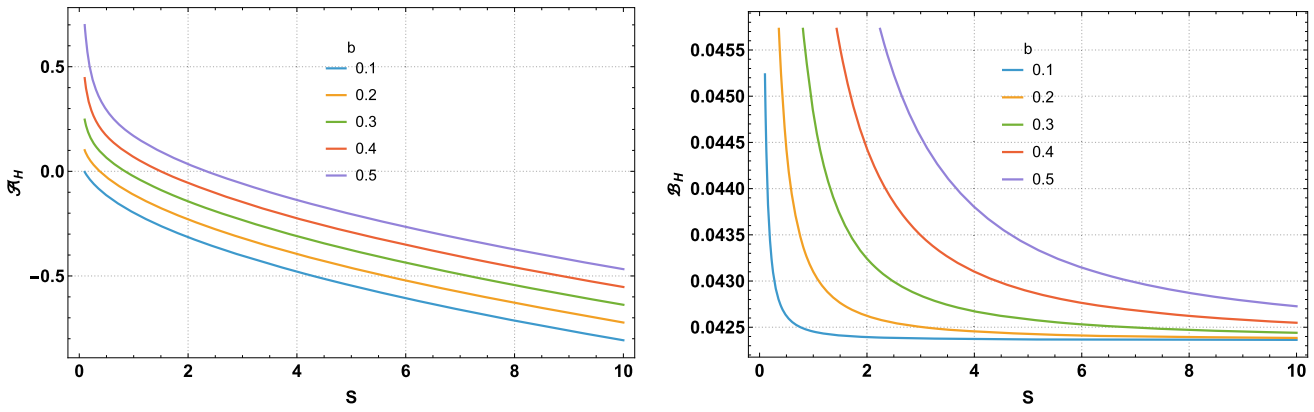

Fig. 8 Behavior of the intensive thermodynamic variables $\mathcal{A}_H$ and $\mathcal{B}_H$ as a function of entropy S for different values of CoS parameter b

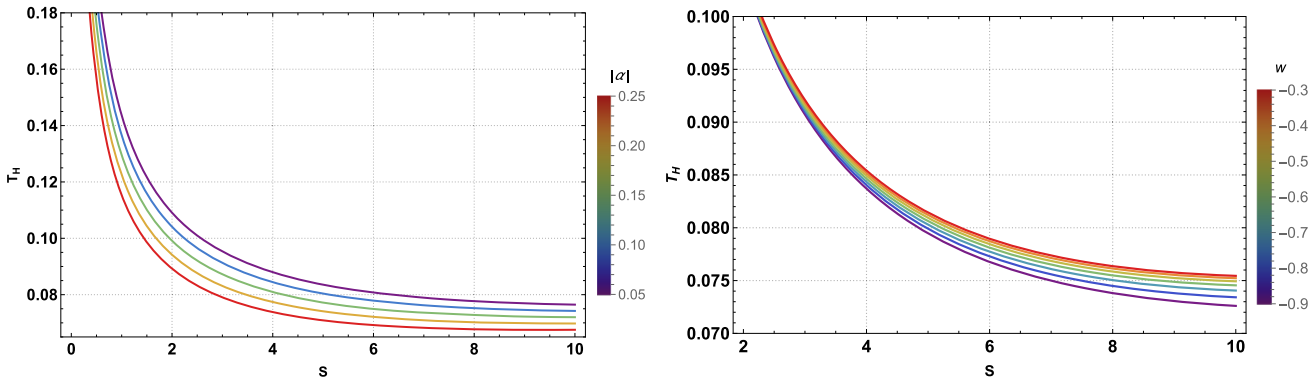

Fig. 9 Behavior of the temperature T_H given in Eq. (32) as a function of entropy for different values of CoS parameter α and state parameter w. Here, we set $\mathrm{N} = 0.01,\ P = 0.01$

controlled setup allows us to probe, in a clean way, how variations in α and ω modify the thermodynamic profile of the BH system. The figure reveals that both α and ω exert a pronounced influence on the temperature-entropy relation. The parameter α encodes deviations from standard general relativity, with nonzero values reflecting corrections from the underlying modified gravity framework. As α varies, one observes notable shifts in the temperature curve, indicating that the thermal properties of the BH are highly sensitive to these gravitational modifications. In this sense, α acts as a probe of the microscopic structure of spacetime, influencing how the BH exchanges energy and evolves thermodynamically. On the other hand, the parameter ω, representing the equation of state of the surrounding matter content, determines the effective type of energy or fluid interacting with the BH. Different values of ω correspond to distinct physical regimes, such as quintessence-like matter, cosmological constant-dominated phases, or other exotic energy components. The resulting modifications in the $T_H(S)$ profile illustrate how the presence of various forms of matter alters the BH's equilibrium properties and phase structure. The interplay between α and ω enriches the thermodynamic behavior, revealing a spectrum of possible stability regimes and phase transition patterns. In particular, the appearance of extrema or turning points in the $T_H(S)$ curves signals potential phase transitions, analogous to those observed in Van der Waals-like systems. These transitions demarcate stable and unstable thermodynamic branches, thereby providing a window into the microscopic degrees of freedom associated with the BH horizon. Overall, the temperature-entropy relationship displayed in Fig. 9 offers valuable insights into the thermal stability and phase structure of BHs within the framework of modified gravity theories and extended thermodynamics. It underscores how both gravitational corrections (through α) and matter content (through ω) intricately shape the thermodynamic landscape of BHs, highlighting the deep connections between fundamental theory, horizon thermodynamics, and the macroscopic behavior of these extreme astrophysical objects.

In addition, the thermodynamic volume of the BH in terms of horizon can be computed as

$$V = \left(\frac{\partial M}{\partial P}\right) = \frac{4\pi r_+^3}{3} \Rightarrow r_+ = (3V/4\pi)^{1/3}. \tag{33}$$

Hence, the Hawking temperature given in Eq. (8) as a function of the BH volume V reads as,

$$\begin{aligned} T = \frac{1}{4\pi}\Bigg[& \left(\frac{4\pi}{3V}\right)^{1/3} - |\alpha|\, b^2 \Bigg\{ \left(\frac{4\pi}{3V}\right) {}_2F_1\left(-\tfrac{1}{2}, -\tfrac{1}{4}, \tfrac{3}{4}, \right. \\ & \left. -\left(\frac{3\,V}{4\,\pi\, b^3}\right)^{4/3}\right) + \frac{2}{3\,b^4}\left(\frac{3V}{4\pi}\right)^{1/3} {}_2F_1 \\ & \left(\tfrac{1}{2}, \tfrac{3}{4}, \tfrac{7}{4}, -\left(\frac{3V}{4\pi b^3}\right)^{4/3}\right)\Bigg\} \\ & + 3w\,\mathrm{N}\left(\frac{4\pi}{3V}\right)^{(3w+2)/3} + 8\pi\, P\left(\frac{3V}{4\pi}\right)^{1/3}\Bigg] \end{aligned} \tag{34}$$

In order to get the inversion temperature, one can use its definition [62,88–90], so that

$$T_i = V\left(\frac{\partial T}{\partial V}\right)_{P,|\alpha|,b,\mathrm{N}}. \tag{35}$$

By using Eq. (34) and computing the inversion temperature, one arrives

$$\begin{aligned} T_i = & -\frac{1}{9}\left(\frac{3V}{4\pi}\right)^{-\frac{1}{3}} + \frac{|\alpha| b^2}{3}\left(\frac{3V}{4\pi}\right)^{-1} {}_2F_1 \\ & \left(-\frac{1}{2}, -\frac{1}{4}, \frac{3}{4}, -\frac{\left(\frac{3V}{4\pi}\right)^{\frac{4}{3}}}{b^4}\right) \\ & + \frac{4|\alpha|}{21b^6}\left(\frac{3V}{4\pi}\right)^{\frac{5}{3}} {}_2F_1\left(\frac{3}{2}, \frac{7}{4}, \frac{11}{4}, -\frac{\left(\frac{3V}{4\pi}\right)^{\frac{4}{3}}}{b^4}\right) \\ & - \frac{1}{3}Nw(3w+2)\left(\frac{3V}{4\pi}\right)^{-\frac{3w+2}{3}} + \frac{8\pi P}{9}\left(\frac{3V}{4\pi}\right)^{\frac{1}{3}} \end{aligned} \tag{36}$$

In terms of horizon radius r_+, the inversion temperature canbe rewritten as,

$$\begin{aligned} T_i = & -\frac{1}{9r_+} + \frac{|\alpha| b^2}{3r_+^3} {}_2F_1\left(-\frac{1}{2}, -\frac{1}{4}, \frac{3}{4}, -\frac{r_+^4}{b^4}\right) \\ & + \frac{4|\alpha| r_+^5}{21b^6} {}_2F_1\left(\frac{3}{2}, \frac{7}{4}, \frac{11}{4}, -\frac{r_+^4}{b^4}\right) \\ & - \frac{1}{3}\,\mathrm{N}\, w\,(3w+2)\, r_+^{-(3w+2)} + \frac{8\pi P r_+}{9} \end{aligned} \tag{37}$$

From expressions (36) or (37), we observe that the inversion temperature is modified by the CoS parameters ($|\alpha|$, b) and the QF parameters (N, w).

Finally, subtracting Eqs. (8) and (37), one gets

$$\begin{aligned} \Delta T = T_i - T = & -\left(\frac{1}{9} + \frac{1}{4\pi}\right)\frac{1}{r_+} + |\alpha|\, b^2 \\ & \times \left(\frac{1}{3} + \frac{1}{4\pi}\right)\frac{1}{r_+^3} {}_2F_1\left(-\frac{1}{2}, -\frac{1}{4}, \frac{3}{4}, -\frac{r_+^4}{b^4}\right) \\ & + \frac{|\alpha|\, r_+}{6\,\pi\, b^2} {}_2F_1\left(\frac{1}{2}, \frac{3}{4}, \frac{7}{4}, -\frac{r_+^4}{b^4}\right) \\ & + \frac{4\,|\alpha|\, r_+^5}{21\, b^6} {}_2F_1\left(\frac{3}{2}, \frac{7}{4}, \frac{11}{4}, -\frac{r_+^4}{b^4}\right) + \mathrm{N} r_+^{-(3\,w+2)} \\ & \times \left[-\frac{1}{3}\,w\,(3\,w+2) - \frac{3\,w}{4\,\pi}\right] + P\, r_+\left(\frac{8\pi}{9} - 2\right) \end{aligned} \tag{38}$$

For a particular state parameter, $w = -2/3$, we find

$$\begin{aligned} \Delta T = & -\left(\frac{1}{9} + \frac{1}{4\pi}\right)\frac{1}{r_+} + |\alpha|\, b^2 \\ & \times \left(\frac{1}{3} + \frac{1}{4\pi}\right)\frac{1}{r_+^3} {}_2F_1\left(-\frac{1}{2}, -\frac{1}{4}, \frac{3}{4}, -\frac{r_+^4}{b^4}\right) \\ & + \frac{|\alpha|\, r_+}{6\,\pi\, b^2} {}_2F_1\left(\frac{1}{2}, \frac{3}{4}, \frac{7}{4}, -\frac{r_+^4}{b^4}\right) \\ & + \frac{4\,|\alpha|\, r_+^5}{21\, b^6} {}_2F_1\left(\frac{3}{2}, \frac{7}{4}, \frac{11}{4}, -\frac{r_+^4}{b^4}\right) \\ & + \mathrm{N}\,\frac{2}{4\,\pi} + P\, r_+\left(\frac{8\pi}{9} - 2\right) \end{aligned} \tag{39}$$

From the above analysis, it is evident that the Hawking or BH temperature exhibits a form significantly different from that of the inversion temperature, which arises when the J-T expansion coefficient of the system vanishes. These two are generally not equal and describe very different physical processes:

- The Hawking temperature is associated with the thermal radiation emitted by a BH due to quantum effects near the event horizon. In contrast, the inversion temperature arises from the J–T expansion in extended BH thermodynamics, defined as the temperature at which the J–T coefficient vanishes.
- The Hawking temperature governs the rate of BH evaporation and is directly related to the surface gravity at the event horizon. On the other hand, the inversion temperature marks the critical point at which the behavior of the BH during an adiabatic expansion at constant enthalpy changes from cooling to heating or vice versa.
- While the Hawking temperature is fundamental for understanding BH radiation and quantum field effects in

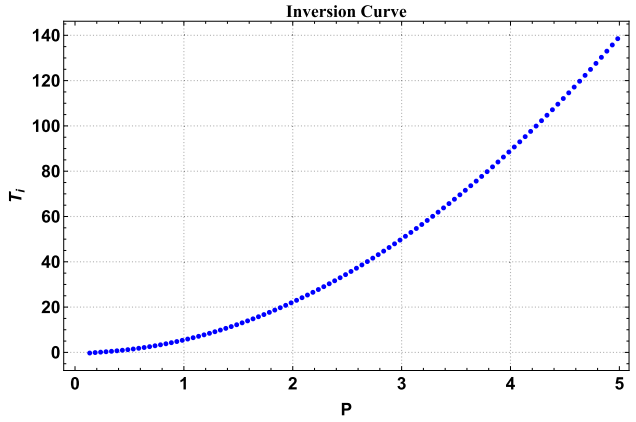

Fig. 10 Inversion curve $P - T_i$ of BH, while fixed $\alpha = 0.05$, $b = 0.2$, $w = -2/3$, $\mathrm{N} = 0.01$

curved space-time, the inversion temperature characterizes the BH as a thermodynamic system in an extended phase space, where the cosmological constant is interpreted as pressure and mass as enthalpy. It reflects a behavior analogous to that of real gases in classical Joule–Thomson expansion processes.

In Fig. 10, we present the inversion curve of the BH, illustrating the regions of cooling and heating. This curve provides insight into the thermodynamic behavior of the BH under a virtual isenthalpic expansion and enables a classification analogous to that of Van der Waals fluids. The region below the inversion curve corresponds to cooling, while the region above it represents heating.

5 Joule–Thomson expansion of AdS BH with CoS and QF

In this section, we will conduct a detailed investigation of the J–T expansion as it applies to the Schwarzschild-AdS BHs with cloud of strings and quintessential-like fluid. The J–T expansion, a classical thermodynamic process, provides insight into the temperature behavior of a system undergoing adiabatic expansion. To draw a parallel with conventional thermodynamics, the J–T expansion typically refers to a throttling process involving a non-ideal fluid, such as a gas or liquid. In this process, the fluid is forced through a valve or porous plug, moving from a region of higher pressure to one of lower pressure. Importantly, this expansion occurs without heat exchange with the surroundings, hence it is adiabatic. While the process is inherently irreversible, the enthalpy of the fluid remains constant throughout, making it an isenthalpic process. This key feature allows for the study of temperature changes that result solely from variations in pressure and volume under constant enthalpy conditions. The change in temperature during the J–T expansion is quantified by the J–T coefficient, denoted by μ, which is defined as the rate of change of temperature T with respect to pressure P at constant enthalpy H [62,88–90]:

$$\mu = \left(\frac{\partial T}{\partial P}\right)_H = \frac{1}{C_P}\left[T\left(\frac{\partial V}{\partial T}\right)_P - V\right]. \tag{40}$$

Here, C_P represents the heat capacity at constant pressure per unit horizon volume of the BH (BH) system. The subscript H indicates that the partial derivative is evaluated along an isenthalpic process. Within the framework of BH thermodynamics in extended phase space, the enthalpy is naturally identified with the BH mass M. This identification is essential because it allows one to treat BHs in close analogy with conventional thermodynamic systems, where enthalpy governs processes involving both heat exchange and mechanical work. The relation under consideration plays a central role in connecting the fundamental thermodynamic variables-temperature T, pressure P, and volume V. Specifically, it allows us to determine how the BH responds under an isenthalpic (constant-mass) expansion or compression. The Joule–Thomson (J–T) coefficient, $\mu = \left(\frac{\partial T}{\partial P}\right)_H$, quantifies this response: a positive J–T coefficient ($\mu > 0$) implies that the system cools upon expansion, meaning that as the BH expands at constant enthalpy, its temperature decreases. A negative J–T coefficient ($\mu < 0$) corresponds to heating upon expansion, where the BH temperature increases under the same conditions. In the BH context, the sign of μ provides direct insight into the interplay between gravitational dynamics and thermodynamic stability. The transition between cooling and heating regimes is marked by an inversion curve, which separates the two behaviors in the T–P plane. Identifying these regimes is crucial, as it reveals whether energy is being absorbed or released by the BH during expansion, thereby enriching our understanding of BH phase transitions and their analogy with real-world fluids. This analysis, illustrated in Fig. 11, demonstrates how the J–T effect serves as a diagnostic tool in extended BH thermodynamics. It not only uncovers the thermodynamic behavior of BHs under isenthalpic processes but also establishes a bridge between classical fluid systems and gravitational thermodynamics, highlighting deep connections between microphysics, horizon geometry, and macroscopic stability.

By applying this formalism to Schwarzschild-AdS BH with CoS and QF, we aim to gain a deeper understanding of their thermodynamic behavior under J–T expansion. So with respect to Eq. (40), we obtain J–T coefficient as,

$$\mu = \frac{\mathrm{A}}{\mathrm{B}}, \tag{41}$$

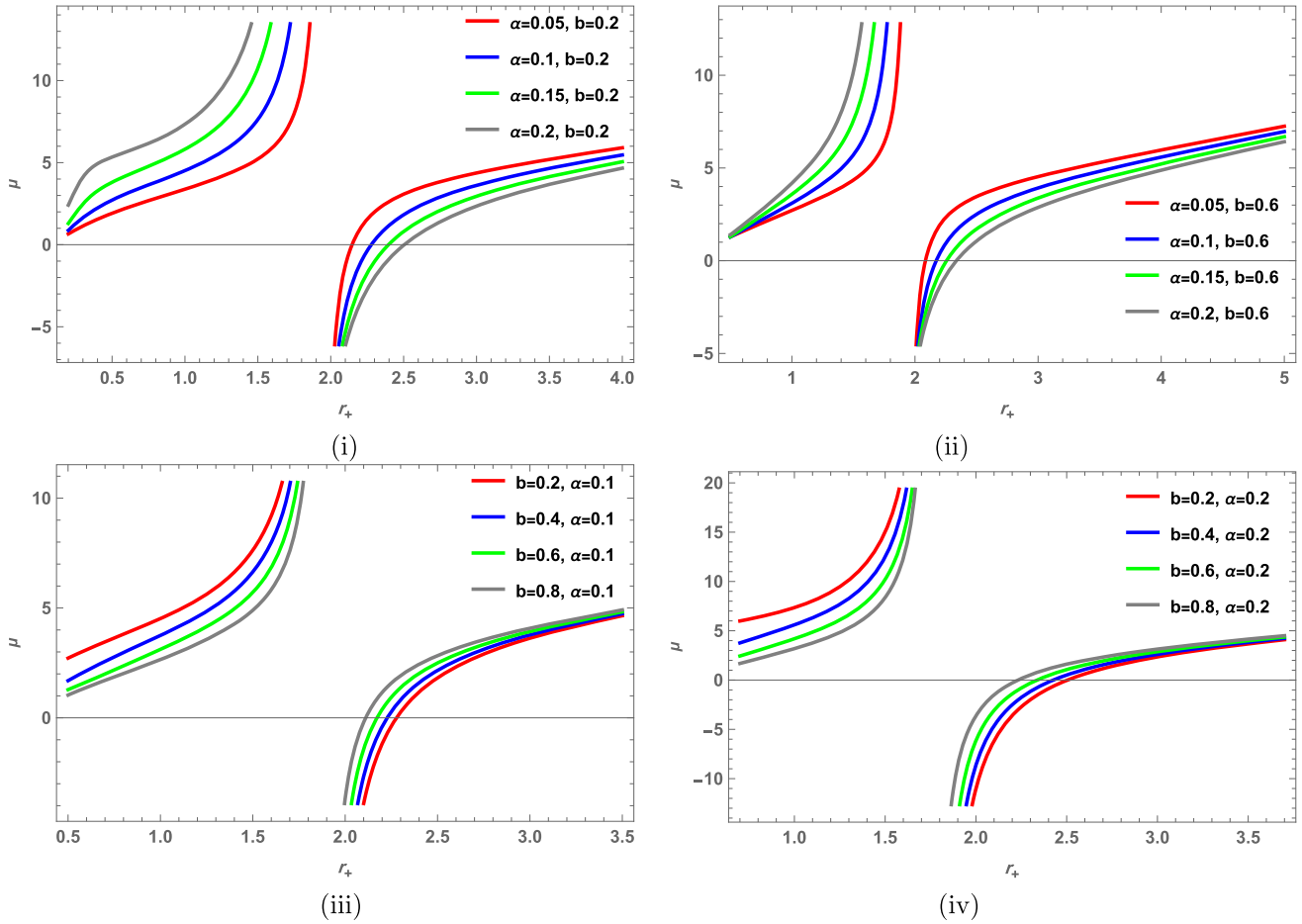

Fig. 11 Profile of J–T coefficient as a function of entropy for fixed parameters $N = 0.01$, P=0.01 and $w = -\frac{2}{3}$, plotted for various values of the parameters α and b. The figure illustrates how changes in α and b influence the thermodynamic behavior and inversion points of the J–T expansion

where we have defined

$$\mathrm{A} = \frac{2r_+\left(|\alpha|\left(-14b^4r_+^4\,{}_2F_1\left(\frac{1}{2},\frac{3}{4};\frac{7}{4};-\frac{r_+^4}{b^4}\right)+18r_+^7\,{}_2F_1\left(\frac{3}{2},\frac{7}{4};\frac{11}{4};-\frac{r_+^4}{b^4}\right)-63b^8\,{}_2F_1\left(-\frac{1}{2},-\frac{1}{4};\frac{3}{4};-\frac{r_+^4}{b^4}\right)\right)+21b^6r_+^2(1-8\pi Pr_+^2)\right)}{21b^4\left(|\alpha|\left(3b^4\,{}_2F_1\left(-\frac{1}{2},-\frac{1}{4};\frac{3}{4};-\frac{r_+^4}{b^4}\right)+2r_+^3\,{}_2F_1\left(\frac{1}{2},\frac{3}{4};\frac{7}{4};-\frac{r_+^4}{b^4}\right)\right)-3b^2r_+^2(-2Nr_++8\pi Pr_+^2+1)\right)}$$

$$\mathrm{B} = \frac{b^2r_+\sqrt{\frac{r_+^4}{b^4}+1}\left(3Nw(3w+5)+4(4\pi Pr_+^2+1)r_+^{3w+1}\right)-2|\alpha|(3b^4+2r_+^4)r_+^{3w}}{|\alpha|(3b^4+r_+^4)r_+^{3w}+b^2r_+\sqrt{\frac{r_+^4}{b^4}+1}\left((8\pi Pr_+^2-1)r_+^{3w+1}-3Nw(3w+2)\right)}. \tag{42}$$

From expression (41), we observe that the coefficient of J–T expansion is modified by the CoS parameters ($|\alpha|$, b) and the QF parameters (N, w). The J–T coefficient determines whether a BH heats or cools during an isenthalpic (i.e., constant mass or enthalpy) expansion. When $\mu > 0$, the BH undergoes cooling as the pressure decreases. Conversely, if $\mu < 0$, the BH heats up during the expansion.

6 Conclusion

In this paper, the analysis of the Schwarzschild-AdS BH surrounded by a cloud of strings and a quintessential-like fluid reveals that the thermodynamic behavior of the system is profoundly influenced by the parameters associated with the external matter fields and the AdS background. By interpreting the BH mass as enthalpy within the extended phase space formalism and associating the cosmological constant with thermodynamic pressure, we derived explicit expressions for

the mass, Hawking temperature, Gibbs free energy, and internal energy, all of which exhibit nontrivial dependence on the cloud of strings parameters (α, b), the quintessence parameters (N, w), and the pressure P. Also, we know that the zero-temperature points corresponding to divergence in the J–T coefficient, marking critical boundaries between heating and cooling phases in expansion or compression processes. For the horizon radii, the thermal curves reveal strong sensitivity to the microphysical parameters, indicating that the presence of the CoS and QF significantly alters near-horizon thermodynamics, while for large BHs these effects become subdominant, leading to a universal asymptotic thermal behavior. The Gibbs free energy analysis, as its dependence on r_+ illustrates potential phase transitions characterized in $F(r_+)$, indicative of first-order or higher-order critical phenomena. In this context, the study of thermodynamics suggests the presence of phase transitions between distinct equilibrium configurations. Also, the internal energy structure underscores the role of external fields in shaping the BH's energetics, give more explanation of the coupling between gravitational, matter, and cosmological contributions that generates a thermodynamic phase space.

The stability analysis of Schwarzschild-AdS BHs in the presence of a cloud of strings and a quintessential-like fluid, based on the behavior of the specific heat C_p, reveals a rich thermodynamic structure influenced by the parameters (α, b) and (N, w). The explicit expressions derived from the Hawking temperature and entropy demonstrate that divergences in C_p occur at certain critical horizon radii, signaling second-order phase transitions where the BH undergoes qualitative thermodynamic changes. Also, cases with $C_p > 0$ correspond to thermally stable configurations capable of sustaining equilibrium under small perturbations, whereas $C_p < 0$ indicates instability, a behavior common in BH thermodynamics.

The thermodynamic geometry results show that the Ruppeiner curvature scalar R_R for the Schwarzschild-AdS BH with a cloud of strings and a quintessential-like fluid provides a clear geometric signature of its phase structure and microscopic behavior. The calculated R_R diverges exactly at the points where the specific heat changes sign, confirming that phase transitions identified through standard thermodynamic analysis have a direct correspondence in the geometric description of the state space. The sign of R_R distinguishes between dominant repulsive ($R_R > 0$) or attractive ($R_R < 0$) microscopic interactions, and both its sign and magnitude are found to be strongly affected by the parameters α and N, representing the string cloud and quintessence-like fluid respectively. This demonstrates that external matter fields can significantly modify the BH's effective microscopic interaction landscape. In the limit of large entropy, R_R approaches zero, indicating that the system's microstructure tends toward ideal gas-like behavior, reinforcing the view that the geometric approach not only complements but deepens the thermodynamic stability analysis.

The results demonstrate that the inversion temperature of a Schwarzschild-AdS BH is significantly influenced by the presence of a cloud of strings (CoS) and a quintessence-like fluid (QF). By extending the first law of BH thermodynamics to include the parameters ($|\alpha|$, b) for the CoS and (N, w) for the QF, the derived expressions reveal how these additional components modify both the Hawking temperature and the inversion temperature compared to the standard AdS case. The analysis tests and shows how variations in these parameters shift the inversion curve, altering the critical points at which the BH transitions between heating and cooling during the Joule–Thomson expansion. In particular, the difference ΔT between the inversion and Hawking temperatures highlights the distinct thermodynamic response induced by CoS and QF effects, with the case $w = -2/3$ providing a simplified example where the modifications become more transparent. This indicates that the coupling of BHs with such external fields can profoundly reshape their thermal phase structure.

The results of J–T expansion analysis reveal that the Schwarzschild-AdS BH with a cloud of strings and a quintessential-like fluid exhibits a distinct dependence of its cooling-heating behavior on the parameters α and b. The explicit form of the J–T coefficient μ shows that variations in these parameters shift the inversion points, thereby altering the regions where the BH cools ($\mu > 0$) or heats ($\mu < 0$) during isenthalpic expansion. As illustrated , increasing α generally enhances the cooling region, while changes in b influence both the magnitude and location of the inversion temperature. Also, this indicates that the interplay between the string cloud density, the nonlinear electromagnetic field strength, and the quintessential fluid significantly affects the thermodynamic response of the system, offering valuable insights into the control of phase behavior in extended BH thermodynamics.

Overall, we have seen that within the extended phase space, the additional geometric components-such as CoS and QF modify the thermodynamic quantities, phase transitions, and the J–T expansion behavior. The altered geometry has direct implications for observables such as the photon sphere, the innermost stable circular orbit, and the size of the BH shadow. Precision imaging with the Event Horizon Telescope or future high-resolution instruments could, in principle, place constraints on these modifications. Accretion processes and X-ray spectra, including quasi-periodic oscillations and iron-line features, are likewise sensitive to such changes, offering another possible observational window. Gravitational-wave astronomy provides a further avenue, as the presence of string clouds and quintessence alters quasi-normal mode spectra and inspiral phasing. Although such deviations may be subtle, next-generation detectors could

reach the sensitivity needed to probe them. Modified thermodynamic properties also influence Hawking evaporation, which has important implications for the evolution and lifetime of primordial BHs. In the cosmological context, the QF must be compatible with large-scale dark energy constraints. Any discrepancy between local BH parameters and cosmological measurements could signal novel couplings or screening mechanisms. From a holographic perspective, the phase transitions of these BHs may be interpreted as duals of thermal transitions in strongly coupled field theories. Such analogies provide speculative models for early-Universe reheating processes or for the dynamics of hidden sectors. Primordial BHs forming in environments dominated by quintessence or string-like matter would evolve differently, potentially affecting constraints from the cosmic microwave background and nucleosynthesis. Theoretical implications are equally significant. The cloud of strings and quintessence parameters effectively act as additional hairs, challenging the strict formulation of the no-hair paradigm and motivating generalizations in modified gravity frameworks. The extended first law of BH thermodynamics acquires new conjugate variables associated with these parameters, refining the thermodynamic description. These modifications may also encode information about the microscopic structure of BH entropy, suggesting a possible connection to statistical models or string-inspired microstates [77,91,92]. Future investigations should focus on computing quasinormal modes, performing ray-tracing simulations of disk spectra and shadows, and studying evaporation signatures for primordial BHs. Such efforts would enable direct comparison with astrophysical and cosmological observations. In summary, this framework not only enriches the thermodynamic structure of AdS BHs but also establishes potential links to observational tests, cosmological implications, and theoretical extensions of gravity.

Acknowledgements We would like to sincerely thank the reviewers for their valuable comments and suggestions, which have greatly improved the quality of this work. F.A. acknowledges the Inter University Centre for Astronomy and Astrophysics (IUCAA), Pune, India, for granting a visiting associateship.

Data Availability Statement This manuscript has no associated data [Author's comment: Data sharing not applicable since no datasets were generated or analyzed in this manuscript].

Code Availability Statement This manuscript has no associated code/software [Author's comment: No new code/software were developed or generated in this manuscript].

Funded by SCOAP[3].

References

1. J.D. Bekenstein, Phys. Rev. D **7**, 2333 (1973)
2. J.D. Bekenstein, Phys. Rev. D **9**, 3292 (1974)
3. S.W. Hawking, Commun. Math. Phys. **43**, 199 (1975)
4. S.W. Hawking, Phys. Rev. D **13**, 191 (1976)
5. S.W. Hawking, D.N. Page, Commun. Math. Phys. **87**, 577 (1983)
6. J.M. Bardeen, B. Carter, S.W. Hawking, Commun. Math. Phys. **31**, 161 (1973)
7. G.W. Gibbons, S.W. Hawking, Phys. Rev. D **15**, 2752 (1977)
8. D. Kubiznak, R.B. Mann, JHEP **033**, 1207 (2012)
9. T. Padmanabhan, Class. Quantum Gravity **21**, 4485 (2004)
10. Y.S. Myung, Phys. Rev. D **77**, 104007 (2008)
11. P.C.W. Davies, Class. Quantum Gravity **6**, 1909 (1989)
12. S. Sumati, S. Kristin, M.W. Donald, Phys. Rev. Lett. **86**, 5231 (2001)
13. Z. De-Cheng, Z.J. Shao, W. Bin, Phys. Rev. D **89**, 044002 (2014)
14. A. Sahay, T. Sarkar, G. Sengupta, JHEP **1004**, 118 (2010)
15. J.M. Maldacena, Adv. Theor. Math. Phys. **2**, 231 (1998)
16. S.W. Hawking, D.N. Page, Math. Phys **87**, 577 (1983)
17. Ch. Niu, Y. Tian, X.-N. Wu, Phys. Rev. D **85**, 024017 (2012)
18. D. Kubiznak, R.B. Mann, JHEP **07**, 033 (2012)
19. S. Gunasekaran, R.B. Mann, D. Kubiznak, JHEP **11**, 110 (2012)
20. A. Chamblin, R. Emparan, C.V. Johnson, R.C. Myers, Phys. Rev. D **60**, 064018 (1999)
21. A. Chamblin, R. Emparan, C.V. Johnson, R.C. Myers, Holography. Phys. Rev. D **60**, 104026 (1999)
22. S. Gunasekaran, R.B. Mann, D. Kubizňák, JHEP **1211**, 110 (2012)
23. N. Altamirano, D. Kubizňák, R.B. Mann, Phys. Rev. D **88**, 101502 (2013)
24. N. Altamirano, D. Kubizňák, R.B. Mann, Z. Sherkatghanad, Class. Quantum Gravity **31**, 042001 (2014)
25. D. Kubizňák, R.B. Mann, M. Teo, Class. Quantum Gravity **34**, 063001 (2017)
26. C.V. Johnson, Class. Quantum Gravity **31**, 205002 (2014)
27. S.W. Wei, Y.X. Liu, arXiv:1605.04629
28. D.J. Gogoi, P. Hazarika, J. Bora, R. Changmai, Fortsch. Phys. **73**, e70004 (2025)
29. R.-B. Wang, S.-J. Ma, L. You, Y.-C. Tang, Y.-H. Feng, X.-R. Hu, J.-B. Deng, Eur. Phys. J. C **84**, 1161 (2024)
30. A. Ashraf, A. Ditta, A. Bouzenada, M. Aslam, P. Channuie, F. Atamurotov, M.Y. Malik, Eur. Phys. J. C **85**, 383 (2025)
31. T. Shigemura, K. Shimizu, S. Sugishita, D. Takeda, T. Yoda, J. High Energy Phys. **2025**, 69 (2025)
32. E. Dai, F. Javed, A. Waseem, M. Alosaimi, R.M. Zulqarnain, Phys. Dark Univ. **49**, 102014 (2025)
33. A. Ditta, F. Javed, A. Bouzenada, G. Mustafa, A. Mahmood, F. Atamurotov, V. Khamidov, J High Energy Astrophys. **45**, 62 (2025)
34. G. Fatima, F. Javed, A. Waseem, B. Almutairi, G. Mustafa, F. Atamurotov, E. Güdekli, Phys. Dark Univ. **47**, 101820 (2025)
35. F. Javed, A. Waseem, P. Channuie, G. Mustafa, T. Muhammad, E. Güdekli, Phys. Dark Univ. **47**, 101766 (2025)
36. F. Javed, G. Fatima, G. Mustafa, S.K. Maurya, B. Almutairi, Phys. Dark Univ. **46**, 101677 (2024)
37. G. Mustafa, F. Javed, S.K. Maurya, S. Alkarni, O. Donmez, A. Cilli, E. Güdekli, J High Energy Astrophys. **44**, 437 (2024)
38. A. Al-Badawi, F. Ahmed, İ Sakallı, Eur. Phys. J. C **85**, 660 (2025)

39. F. Ahmed, A. Al-Badawi, İ Sakallı, Nucl. Phys. B **1017**, 116951 (2025)
40. Ö. Ökcü, E. Aydiner, Eur. Phys. J. C **77**, 24 (2017)
41. Ö. Ökcü, E. Aydiner, Eur. Phys. J. C **78**, 123 (2018)
42. R. D'Almeida, K.P. Yogendran, arXiv:1802.05116
43. H. Ghaffarnejad, E. Yaraie, M. Farsam, Int. J. Theor. Phys. **57**, 1671 (2018)
44. S. Wei, L. Yu-Xiao, B.M. Robert, Phys. Rev. Lett. **129**, 191101 (2022)
45. N. Bai, L. Lei, T. Jun, Phys. Rev. D **107**, 064015 (2023)
46. J. Sadeghi, S.N. Gashti, M.R. Alipour, M.A.S. Afshar, Ann. Phys. (NY) **455**, 169391 (2023)
47. D. Wu, Phys. Rev. D **108**, 084041 (2023)
48. D. Wu, W.S. Qing, Phys. Rev. D **107**, 084002 (2023)
49. D. Wu, S.-Y. Gu, X.-D. Zhu, Q.-Q. Jiang, S.-Z. Yang, J. High Energy Phys. **2024**, 213 (2024)
50. J. Sadeghi, M.R. Alipour, S.N. Gashti, M.A.S. Afshar, Chin. Phys. C **48**, 115115 (2024)
51. D. Wu, Eur. Phys. J. C **83**, 589 (2023)
52. S.N. Gashti, B. Pourhassan, I. Sakalli, Eur. Phys. J. C **85**, 305 (2025)
53. S.N. Gashti, J. Hologr. Appl. Phys. **5**(2), 72–85 (2025)
54. J.X. Mo, G.Q. Li, S.Q. Lan, X.B. Xu, Phys. Rev. D **98**, 124032 (2018)
55. M. Chabab, H. El Moumni, S. Iraoui, K. Masmar, S. Zhizeh, Lett. High Energy Phys. **02**, 05 (2018)
56. A. Rizwan, C. L., N. Kumara A.,D. Vaid, K.M. Ajith, Int. J. Mod. Phys. A **33**, 1850210 (2019)
57. J. Pu, S. Guo, Q.Q. Jiang, X.T. Zu, Chin. Phys. C **44**, 035102 (2020)
58. D.M. Yekta, A. Hadikhani, Ö. Ökcü, Phys. Lett. B **795**, 521 (2019)
59. S. Guo, J. Pu, Q.Q. Jiang, arXiv:1905.03604 [gr-qc]
60. A. Cisterna, S.Q. Hu, X.M. Kuang, Phys. Lett. B **797**, 134883 (2019)
61. D.V. Singh, S. Siwach, Phys. Lett. B **808**, 135658 (2020)
62. C. Li, P. He, P. Li, J.B. Deng, Gen. Relativ. Gravit. **52**, 50 (2020)
63. J.X. Mo, G.Q. Li, Class. Quantum Gravity **37**, 045009 (2020)
64. S.Q. Lan, Phys. Rev. D **98**, 084014 (2018)
65. J. Barrientos, J. Mena, Phys. Rev. D **106**, 044064 (2022)
66. T. Huo, C. Liu, Int. J. Theor. Phys. **64**, 173 (2025)
67. A. Waseem, F. Javed, G. Mustafa, S.K. Maurya, F. Atamurotov, M. Shrahili, Ann. Phys. (NY) **480**, 170087 (2025)
68. M. Zhang, C.-M. Zhang, D.-C. Zou, R.-H. Yue, Nucl. Phys. B **973**, 115608 (2021)
69. D. Kastor, S. Ray, J. Traschen, Class. Quantum Gravity **26**, 195011 (2009)
70. P.S. Letelier, Phys. Rev. D **20**, 1294 (1979)
71. M. Barriola, A. Vilenkin, Phys. Rev. Lett. **63**, 341 (1989)
72. G. Alencar, R.R. Landim, R.N. Costa Filho, Phys. Dark Univ. **49**, 102031 (2025)
73. S. Perlmutter et al. (Supernova Cosmology Project), Astrophys. J. **517**, 565 (1999)
74. N. Aghanim et al. (Planck), Astron. Astrophys. **641**, A6 (2020)
75. Y. Akrami et al. (Planck), Astron. Astrophys. **641**, A10 (2020)
76. V.V. Kiselev, Class. Quantum Gravity **20**, 1187 (2003)
77. A. Kumar, Q. Wu, T. Zhu, S.G. Ghosh, arXiv:2508.02768 [gr-qc]
78. F. Ahmed, S.N. Gashti, A. Bouzenada, B. Pourhassan, arXiv:2508.07438 [gr-qc]
79. V.V. Kiselev, Class. Quantum Gravity **20**, 1187 (2003)
80. S. Soham, A. Dutta, S. Gangopadhyay, Eur. Phys. J. C **85**(2), 117 (2025)
81. M.M. Dias e Costa, J. M. Toledo, V.B. Bezerra, Int. J. Mod. Phys. D **28**, 1950074 (2019)
82. M. Shahjalal, Nucl. Phys. B **940**, 63 (2019)
83. S.W. Wei, Y.X. Liu, Phys. Rev. D **90**, 044057 (2014)
84. G. Ruppeiner, Phys. Rev. A **20**, 1608 (1979)
85. F. Weinhold, J. Chem. Phys. **63**, 2479 (1975)
86. B. Pourhassan, S.S. Wani, S. Soroushfar, M. Faizal, J. High Energy Phys. **2021**, 27 (2021)
87. B. Pourhassan, H. Aounallah, M. Faizal, S. Upadhyay, S. Soroushfar, Y.O. Aitenov, S.S. Wani, J. High Energy Phys. **05**, 030 (2022)
88. B.Z. Maytal, A. Shavit, Cryogenics **37**, 33 (1997)
89. S.-Q. Lan, Phys. Rev. D **98**, 084014 (2018)
90. M.R. Alipour, S.N. Gashti, M. Ali, S. Afshar, J. Sadeghi, Gen. Relativ. Gravit. **57**, 61 (2025)
91. C. Wenfu, W. Liu, X. Wu, Gen. Relativ. Gravit. **55**, 120 (2023)
92. S. Qi et al., Phys. Dark Univ. **46**, 101599 (2024)